Chapter 2
An Observational Review of Rotation in A Stars

Abstract Rotation is a key physical process operating in the A stars. Angular rotational velocities reach their maximum at about A5 with some stars rotating at a large fraction of their break-up velocity. Slow rotators are also seen at spectral type A, and these tend to be chemically peculiar. The literature on rotation in the A stars is reviewed, including the mechanisms by which a star's rotation can be braked. For Ap stars, braking is understood, but too few progenitors are observed. For the Am stars, the tidal braking mechanisms proposed in the literature induce mixing that is incompatible with observed abundance anomalies. Unexpectedly, the literature review revealed evidence that A stars *accelerate* for the first third of their main-sequence life, confirming the results of Zorec and Royer (2012). The possibility of determining rotational velocities from the Fourier transforms of *Kepler* light curves is also discussed.

2.1 Introductory Remarks

The stars of spectral type A do not necessarily remain so throughout their life on the main sequence. The principal direction of evolution across the HR diagram for stars at this spectral type is towards cooler temperatures, i.e. to the right (see Fig. 2.1). Thus stars born at late B will evolve to become early-A stars and stars at late A with luminosity class V will become early-F giants. For this reason, and others, a review of the rotational velocities of A stars naturally extends into neighbouring regions of the HR diagram. For reference, the mass of a typical star at A0 is $\sim 2.5\,M_{\odot}$. To aid the reader, Appendix A provides a calibration of spectral type, temperature, photometric indices and colours that has been assembled from the literature.

A-type stars show a range of spectral peculiarities, most common of which are the Am and Ap phenomena. As such, stars without 'abnormal' spectra are referred to as 'normal' stars, even though at some spectral types, normal stars do not constitute the majority. Throughout this review, a normal star simply means not classified as abnormal (mostly Am or Ap) in some way.

The A stars possess a wide range of equatorial rotational velocities, from a few $m\,s^{-1}$ (γ Equ rotates around once per century; Leroy et al. 1994) right up to

S.J. Murphy, *Investigating the A-Type Stars Using Kepler Data*,
Springer Theses, DOI 10.1007/978-3-319-09417-5_2

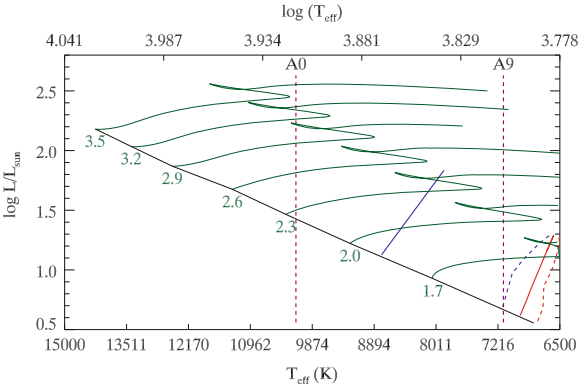

Fig. 2.1 HR diagram covering the late-B to early-F region (spectral types A0 and A9 are delimited). A star at A0 has a surface temperature of ∼10,150 K, and at A9 ∼7,150 K. Evolutionary tracks are plotted in *green*, with their corresponding masses (in $M_\odot$) written just below the zero-age main sequence (*black*). The principal direction of evolution for the B stars is to the right, such that they become A stars. For reference, the δ Sct instability strip's *red* and *blue* edges are plotted as *solid lines*, and the γ Dor strip as *dashed lines*. Tracks were calculated using time-dependent convection (TDC) models, and contributed by A. Grigahcène (priv. comm.)

400 km s^{-1} for the most massive stars (Zorec and Royer 2012). Since many stellar properties are correlated with rotation, stars are commonly described as either 'fast' or 'slow' rotators about a dividing line of 120 km s^{-1}. This line marks the observational limit up to which chemically peculiar A stars are found, as we shall see in this review.

2.2 Velocity Distributions

2.2.1 Is the Distribution Bimodal?

It has long been observed that there is an excess of slow rotators among the A stars. Conti (1965) concluded that at least two separate velocity distributions are represented among the A stars, and that the slow rotators among the late-A stars were the metallic-lined Am stars. Similarly, Wolff (1967) showed that the correlation between chemical peculiarity and rotation in late-B and early-A stars was consistent only with Ap stars being slow rotators, i.e. not fast rotators seen pole-on.

Perhaps the best illustrations of the bimodal nature of the rotational distributions of A stars come from Abt and Morrell (1995) and Zorec and Royer (2012). In the latter, Maxwellians are used to describe the distributions of rotational velocities. From observations in the former it is then clear that at least two Maxwellians are required to describe the distribution empirically (Fig. 2.2), with the slowly rotating

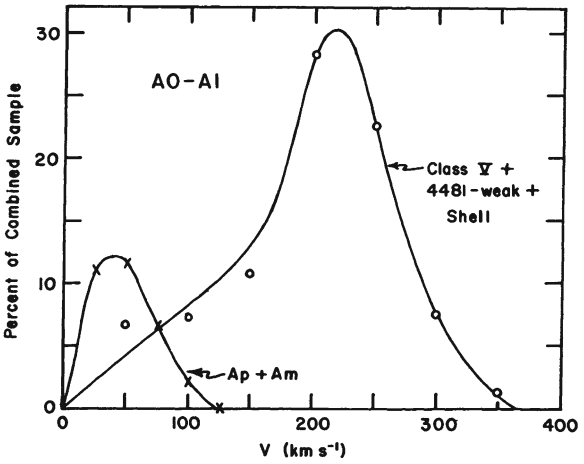

Fig. 2.2 Distributions of equatorial rotational velocities, V, for two samples of A0–A1 stars. The right distribution is for 188 normal class V stars, 58 stars with weak λ4481 lines and five shell stars; the distribution on the left is for 46 Ap+Am stars whose peculiar abundances are thought to be due to diffusion. The areas under the curves are proportional to their relative frequencies in the Bright Star Catalogue. Figure and caption from Abt and Morrell (1995, Fig. 4). Permission obtained from author; reproduced by permission of the AAS

population being chemically peculiar (CP), that is, all Am or Ap stars. It is noteworthy, however, that Preston (1970) argued that if the Ap stars with rotational velocities of years belong to the same slow-rotator distribution, then they are over-represented in observations by an order of magnitude.

Zorec and Royer (2012), on the other hand, clearly showed a slowly rotating population of stars for masses above $\sim 2.5\,M_{\odot}$, *after* removing known CP and close binary stars from their sample (Fig. 2.3). Thus they have found a subsample of slow rotators among the *normal* stars, despite claims that the bimodal distribution for late-B stars can be explained by a set of slowly rotating Ap stars and a set of rapidly rotating, normal B stars (Abt et al. 2002). Either way, one can see that the situation is more complex than a superposition of one or two Maxwellian distributions.

2.2.2 Variations Between Observers

The two most active 'groups' in studying the rotational velocities of A stars in the past two decades have been the Royer group (Royer et al. 2002a, b; Royer et al. 2007; Zorec and Royer 2012), and Abt and his collaborators (Abt and Morrell 1995; Abt 2004, 2009). Here we shall explain the methods and discuss the results of the groups.

Both groups have sufficiently large samples to correct statistically for inclination. Abt's sample is based on the 1,700 northern stars for which half-widths of the

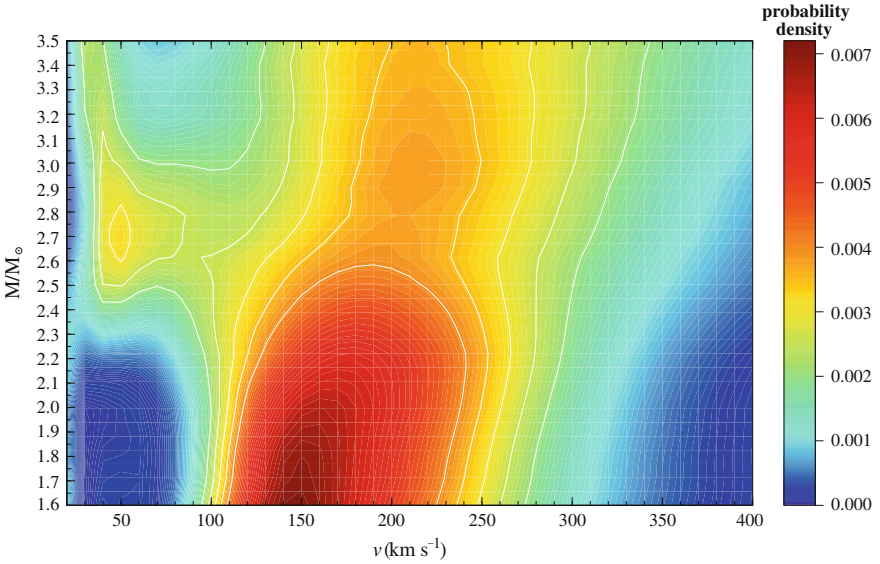

Fig. 2.3 Distribution of true rotational velocities, v, for normal stars as a function of the stellar mass, $M/\mathrm{M}_\odot$. The colour scale represents the density in the one-dimensional normalised distributions. The bluer the region, the smaller the number of stars, and vice-versa for the *red-coloured scale*. *White solid lines* follow iso-density contours. Figure and caption from Zorec and Royer (2012, their Fig. 7). Permission obtained from A&A

Mg II 4481 and Fe I 4476 lines were determined by Abt and Morrell (1995), using the Slettebak system—a catalogue of $v \sin i$ versus FWHM of many lines for late-O to late-F stars—which has seen wide use, but whose $v \sin i$ values are regarded to be slightly underestimated (Royer 2009, and references therein). The more recent papers from the Royer group used a combination of Abt et al.'s (2002) data, with binaries and CP stars removed, and data from Royer et al. (2002a, b), in which rotational velocities were derived for 777 southern stars from Fourier transforms of several line profiles in the 4200–4500 Å range. The magnesium doublet was not chosen by the latter authors because at low rotational velocities the intrinsic separation of the doublet becomes visible and the line width is no longer sensitive to rotational broadening. The error on the Fourier method is judged to be 6 %, and the main difference in rotational velocities between the Abt and Morrell and Royer et al. samples occurs for $v \sin i$ below 25 km s^{-1}. A systematic shift of 5.3 km s^{-1} as well as a 15 % difference in $v \sin i$ is observed between the two samples, which implies, according to Royer et al., that Abt and Morrell's velocities are slightly too low. Abt and Boonyarak (2004) maintain that Abt and Morrell's velocities are valid. Nevertheless, there now exists a 'corrected' version of Abt and Morrell's catalogue, taking into account the underestimation of the Slettebak system, in Royer et al. (2002b). Finally, Royer et al. (2007) note that differences in mean, true equatorial velocities from their method compared

to the literature can reach $\Delta v = 50\,\mathrm{km\,s^{-1}}$. Their thorough comparisons and tests imply the literature values are underestimated.

Even once the differences in $v \sin i$ from different observing methods are taken into account, discrepancies in results still remain. Abt et al. (2002) found that only 0.3 % of B stars have rotational velocities in excess of two-thirds of break-up velocity, whereas Royer et al. (2007) showed a distinctly different case for the B9 stars: approximately 30 % appear to be above the $\Omega/\Omega_c > 2/3$ threshold (Fig. 2.4), where Ω_c is the critical angular velocity corresponding to break-up. An explanation for this difference is that B9 stars are substantially closer to the maximum of Ω/Ω_c at A5 than are the group of Abt et al.'s B stars as a whole. That maximum at A5 is particularly clear in the middle-right panel of Fig. 2.4, where all stars are fast rotators. Closer inspection of some of the numbers in Royer et al. (2007) might reveal another cause of the discrepancies. They only removed 16 CP and 33 close binary stars from

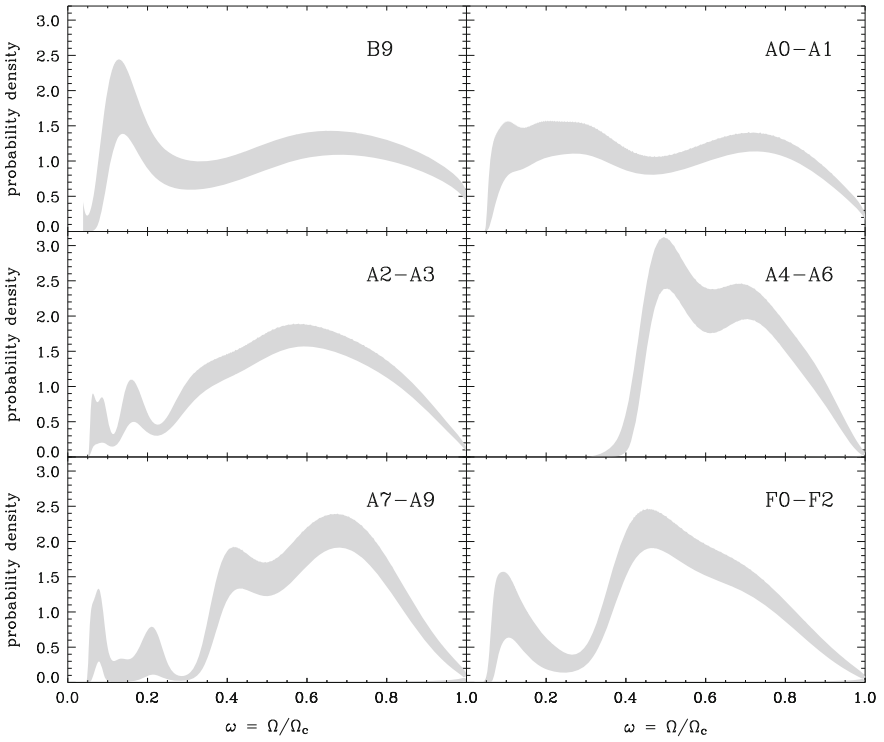

Fig. 2.4 Distributions of angular velocities as a fraction of the critical velocity for breakup , Ω/Ω_c, derived from v distributions in Royer et al. (2007). $\omega = 1$ thus corresponds to break-up. The area under a band over a particular angular velocity interval corresponds to the fraction of stars in that interval. Only the variability band of each probability density function is displayed—the width of the band can be thought of as the size of the error bars, and the computed values lie approximately at the centre of each band. Figure from Royer et al. (2007, their Fig. 10). Permission obtained from A&A

their total of 190 stars in the A7–A9 range. If one assumes all of those close binaries are Am stars (see Sect. 2.4), then they find only a quarter of stars in this range to be Am. Yet it is widely observed that at about A8, Am stars comprise about 50 % of the A-star population (e.g. Smith 1973). One must also consider that Royer et al. are considering luminosity classes IV and V only. The proportion of Am stars increases with age (North 1993; North et al. 1997), but only up to the terminal-age main sequence (TAMS), so Royer et al. are probably not missing many of those. Perhaps their disregard for the more evolved objects, covering ρ Pup stars and metallic A-F giants, makes up some of the deficit and they do not have a strong selection bias.

Alternatively, it is possible that Royer et al. (2007) have isolated in their 'normal slow rotators' subgroup those Ap stars that are yet to develop some chemical peculiarity. Specifically, it takes the cluster Ap SrCrEu stars half of their main-sequence life to reach the same frequency as is observed in field stars (Abt 2009). The ages of Royer, Zorec and Gómez's 'normal slow rotators' subgroup were not determined beyond the fact that they are main-sequence objects, so at least some of them could be Ap progenitors.

To settle the debate, we can refer to comparisons of rotational velocities in two other surveys: Uesugi and Fukuda (1982) and Erspamer and North (2003). The latter two sources are in good agreement with one another. In comparison, the results of Abt and Morrell (1995) are lower, particularly for $v \sin i > 100\,\mathrm{km\,s^{-1}}$, whereas the results of Royer et al. (2002a) are in better agreement. In terms of systematic errors (neglecting sample coverage), all sources are satisfactorily mutually consistent.

2.2.3 Evolution

Since we have just commented on the increase in CP prevalence with age, and slow rotation is correlated with the Am and Ap phenomena, let us review the effect of evolution on A star rotational velocities.

Wolff and Simon (1997) compared the mean rotational velocities of field stars with those of young stars in Orion, the α Per cluster, the Pleiades and the Hyades. They showed that there is no appreciable decline in rotational velocity on the main sequence among the 1.9–2.4 $\mathrm{M}_\odot$ stars, but that for stars between 1.3 and 1.6 $\mathrm{M}_\odot$ the decrease in $v \sin i$ ranges from 30–50 % (Fig. 2.5). If one assumes equal braking rates, the result is explained by the difference in nuclear time-scales between the two mass ranges.

If the coupling between the surface and the interior is sufficiently strong, Wolff and Simon (1997) claim a star will rotate as a solid body. However, how strong is the coupling when stars rotate at a substantial fraction of the break-up velocity? Wolff and Simon used strong coupling as an explanation for the constant velocities of stars above 1.6 $\mathrm{M}_\odot$ during their main-sequence lifetime, but Royer et al. (2007) have shown that the mean value of the fraction of critical angular velocity, Ω / Ω_c, is around 2/3 for A4–A9 stars, and about 1/2 for F0–F2 (Fig. 2.4). It is hard to imagine that these stars rotate as solid bodies , particularly near the end of their main-sequence

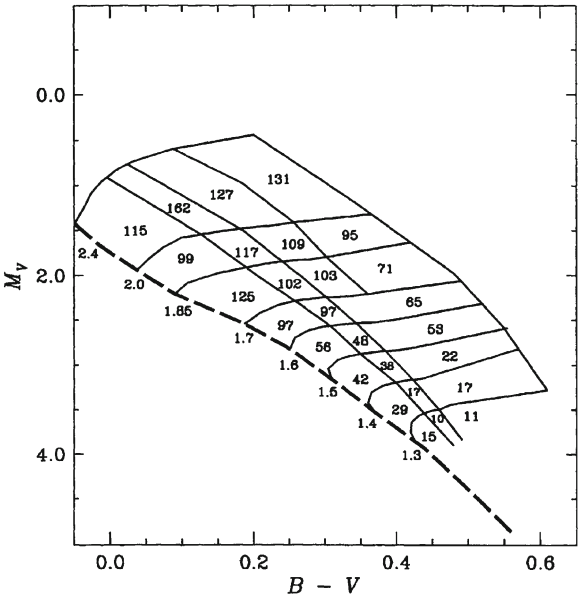

Fig. 2.5 The average rotational velocities of stars as a function of mass and age. The heavy *dashed line* represents the zero-age main sequence (ZAMS). The nearly *horizontal lines* represent evolutionary tracks with the masses indicated just to the left of the ZAMS. The lines nearly parallel to the ZAMS are used to separate the stars into different groups according to the extent of their evolution away from the ZAMS. Numbers enclosed are the average $v \sin i$ for the enclosed populations. Figure and caption from Wolff and Simon (1997, Fig. 3b). Permission obtained from author

lives. Indeed, Zorec and Royer (2012) show that stars of $2.0\,M_\odot$ and higher rotate with more rotational energy at the TAMS than a critical rigid rotator can bear, and must therefore be rotating differentially. Even the Sun rotates differentially and it is a slow rotator, so the rigid rotator hypothesis seems untenable.

How do the observational results of Wolff and Simon (1997), reproduced in Fig. 2.5, here, compare to the more recent ones of Zorec and Royer (2012), who also investigated the evolution of rotational velocities in A stars? The latter authors used $uvby\beta$ photometry and *Hipparcos* parallaxes to determine $T_{\rm eff}$ and $\log L/L_\odot$, and then used stellar evolution models to calculate masses and ages.[1] They found that normal stars in the 2.0–2.4 $M_\odot$ range appear to rotate *more quickly* with time spent on the main sequence ($t_{\rm MS}$). Specifically, they found a monotonic increase in mean age across the 50–110 $\mathrm{km\,s^{-1}}$ velocity interval, suggesting the faster rotators of the interval are older, and implying some sort of spin-up from angular momentum redistribution among the *slow* rotators (Fig. 2.6). The trend diminishes with increasing mass. However, the CP stars belonging to the slow rotator population in any mass range from 2.0 to 3.5 $M_\odot$ showed only slight changes in rotational velocity with age,

[1] Their quoted errors on $T_{\rm eff}$, $L/L_\odot$, $M/M_\odot$, and age were on the order of 2, 15, 3 and 10 %, respectively. Their models are detailed in the two appendices of that paper.

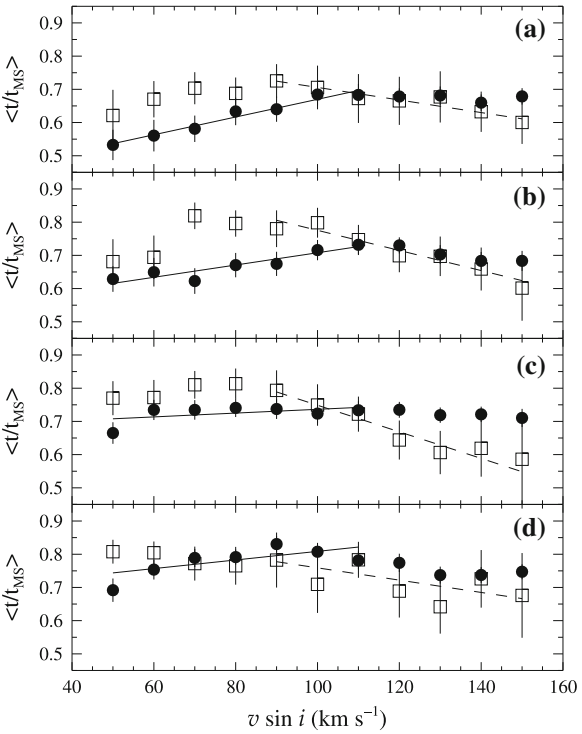

Fig. 2.6 Mean age $\langle t/t_{\rm MS}\rangle$ per bin of $v \sin i$ for different mass intervals: **a** $2 < M/M_\odot < 2.4$; **b** $2.2 < M/M_\odot < 2.6$; **c** $2.35 < M/M_\odot < 2.85$; **d** $2.55 < M/M_\odot < 3.05$. *Filled circles* stand for normal stars, whereas *open squares* represent CP stars. The bins in $v \sin i$ are $40\,\mathrm{km\,s^{-1}}$ wide. *Solid lines* are the results of linear fits on normal stars with $v \sin i \leq 110\,\mathrm{km\,s^{-1}}$ and *dashed lines* the results of the fits for CP stars with $v \sin i \geq 90\,\mathrm{km\,s^{-1}}$. Figure and caption from Zorec and Royer (2012, their Fig. 8). Permission obtained from A&A

and showed moderate decelerations for those CP stars belonging to the fast rotator population (albeit with larger errors).

Zorec and Royer calculated models for a variety of stellar structures, using different approaches to rotation. Specifically, they looked at the cases of rigid and differential rotation for different ZAMS rotation rates. Differential rotation can be either *simple*, where the specific angular momentum, J/M, is lower than the critical value that a *rigid* rotator can possess, or *neat*, where that critical value is exceeded. Their rigid rotator models are two-dimensional and were constructed for $M = 1.5$ and $3.0\,\mathrm{M}_\odot$, conserving total angular momentum throughout the main-sequence phase. Both masses showed only a marginal increase in $v/v_{\rm ZAMS}$ over the first two-thirds of $t_{\rm MS}$, but rapid increases of over 0.4 in $v/v_{\rm ZAMS}$ in the final third (Fig. 2.7). Conversely, stars in the simple differential rotation regime were forecast to show monotonic decreases of 40 % ($1.5\,\mathrm{M}_\odot$ case) or greater ($3\,\mathrm{M}_\odot$ case) over the entire $t_{\rm MS}$.

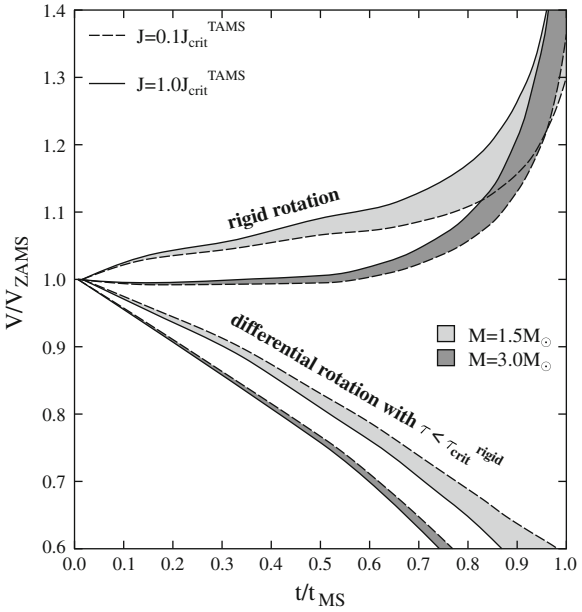

Fig. 2.7 $v/v_{\rm ZAMS}$ ratio of equatorial rotational velocities as a function of the $t/t_{\rm MS}$ ratio in the main sequence for stars with masses $M = 1.5$ & $3\,{\rm M}_{\odot}$. $v_{\rm ZAMS}$ is the equatorial rotational velocity on the ZAMS, t is the stellar age and $t_{\rm MS}$ is the time that a star of given mass M can remain on the main sequence. Two extreme cases are represented: stars evolving as rigid rotators (instantaneous complete angular momentum redistribution) and as differential rotators without any angular momentum redistribution. *Dashed lines* represent the limits for $J/M \rightarrow 0$, while the *solid lines* are for stars that on the ZAMS have a specific angular momentum that in the TAMS becomes a critical one. τ is the ratio of kinetic to gravitational potential energy in the star. Figure and caption from Zorec and Royer (2012, their Fig. 10). Permission obtained from A&A

In the differentially rotating case, the specific angular momentum becomes increasingly centrally condensed, meaning the surface rotational velocity decreases strongly as a function of $t_{\rm MS}$, almost irrespective of mass. The results for differential rotation are fairly independent of the value of J, but by definition rotational velocities become critical in a rigid rotator when $J = J_{\rm crit}^{\rm TAMS}$.

Zorec and Royer then compared their observational results, for which values of J/M were calculated, to their models. They confirmed that their 'low rotational energy regime' assumption, in which differential rotators have less total angular momentum than the critical value for a rigid rotator, is valid. They highlighted that spin-up of surface angular velocities is only possible with differential rotation, where the core is rotating more quickly than the envelope and angular momentum is transported outwards. This is entirely plausible if a star is braked more strongly at the surface during the pre-main sequence phase (due to, say, disc interaction), than at the core. Their observations of rotational velocities increasing in the first third of the main-sequence lifetime (Fig. 2.8) can be explained by a rigid, rapidly rotating core

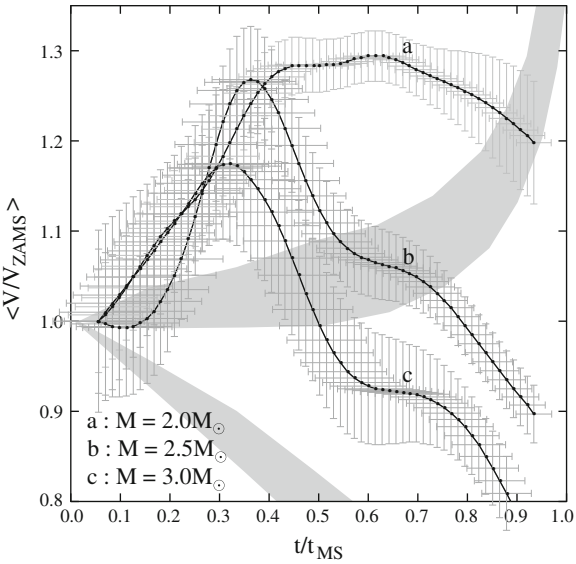

Fig. 2.8 Evolution of the equatorial velocity ratio $\langle v/v_{\rm ZAMS}\rangle$ in the main-sequence lifetime span, where $v_{\rm ZAMS}$ is the true equatorial velocity of stars on the ZAMS. The *shaded regions* correspond to the theoretical evolution of the $v/v_{\rm ZAMS}$ ratios shown in Fig. 2.7 (this document): rigid rotators (*middle*), simple differential rotators (*lower left corner*). Figure and caption from Zorec and Royer (2012, their Fig. 15). Permission obtained from A&A

transferring angular momentum to the surface. The turning point then represents the phase where the core and surface are rotating at the same rate. The more massive stars then decelerate efficiently (possibly as neat differential rotators for cases of high angular momentum) in a way consistent with angular momentum being conserved in shells with no redistribution. The lower ($2.0\,{\rm M}_\odot$) mass stars do not decelerate efficiently and end up with TAMS velocities greater than they were on the ZAMS.

If we investigate the mass range of $\sim$1.8–$2.0\,{\rm M}_\odot$ more closely, we have four information sources that are in agreement. From the observations of Zorec and Royer (2012), we expect an initial spin-up starting at the ZAMS, to a peak in the central third of the main-sequence lifetime, followed by a weaker deceleration in the latter third of the main-sequence band (cf. Fig. 2.8). Inspection of the numbers of Wolff and Simon (1997, cf. Fig. 2.5, here) for this mass range agrees with that prediction, but with a stronger final deceleration than we would expect from Zorec and Royer (2012). A third source of information comes from Erspamer and North (2003), who analysed $v \sin i$ and $\log g$ for a sample of A and F stars using the ELODIE and CORALIE echelle spectrographs and *Hipparcos* data. Their uncertainty of 0.2 dex in $\log g$ is not favourable (though not intrinsically poor, either), and there would be much benefit in having more data, but still the data show an agreement with $v \sin i$ initially increasing and then decreasing in the latter half of the main-sequence band. We illustrate that agreement in Fig. 2.9, which is a replot of their Fig. 14, noting the main-sequence

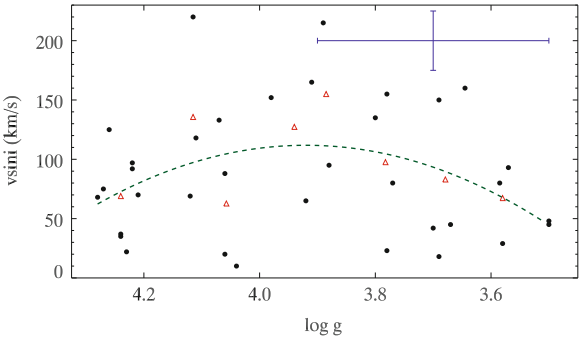

Fig. 2.9 A replot of Fig. 14 of Erspamer and North (2003), showing the variation of $v \sin i$ with $\log g$ over the main-sequence band, which extends from about $\log g = 4.3$ to 3.5 for the 1.8–2.0 $M_\odot$ range. Original data shown as filled *black circles*. Added in the upper right is a typical error bar representing a conservative 0.2 dex in $\log g$ and 25 km s^{-1} in $v \sin i$ (estimated—Erspamer and North do not quote exact errors). The *dashed line* is a second-degree polynomial fit to the data, the significance of which is described in the text. Open *red triangles* represent the binned data

band stretches from about 4.3–3.5 in $\log g$. Here, a second-degree polynomial has been fitted to the data to aid the eye. Although the correlation is not tight ($R^2 = 0.03$ for a second-order polynomial, vs. 0.003 for a straight line), one must consider the large star-to-star variation in $v \sin i$ and the difficulty in obtaining precise $\log g$, which will affect any observational attempt to confirm the result. For this reason, the original data were binned into 0.1-dex bins in $\log g$ and added to Fig. 2.9. This shows a clearer correlation to the fit. Finally, the fourth source is Slettebak (1955), who in his Figure 6 showed mean rotational velocities against spectral type and luminosity class, much like Wolff and Simon (1997) did later, but Slettebak had a coarser grid. Erring strongly on the side of caution, Slettebak did not note the acceleration as astrophysical.

2.2.4 *Inferring Velocity Distributions from Fourier Transforms of Kepler Data*

The rotational velocity distribution of the A stars is well studied, and, as we saw in Sect. 2.2.1, and will continue to discuss later in this chapter, determines the emergence of chemical peculiarities in these stars. Its importance has drawn many studies, both spectroscopic (e.g. Abt and Morrell 1995) and photometric (e.g. Balona 2011). In the latter, Balona used *Kepler* data for several hundred A0–A8 field stars, finding about 8 % of them had light curves resembling those of cool stars with spots. A further 20 % had dominant low frequencies (example provided in Fig. 2.10) that were also attributed to spots or "some other corotating structure". By assuming the dominant

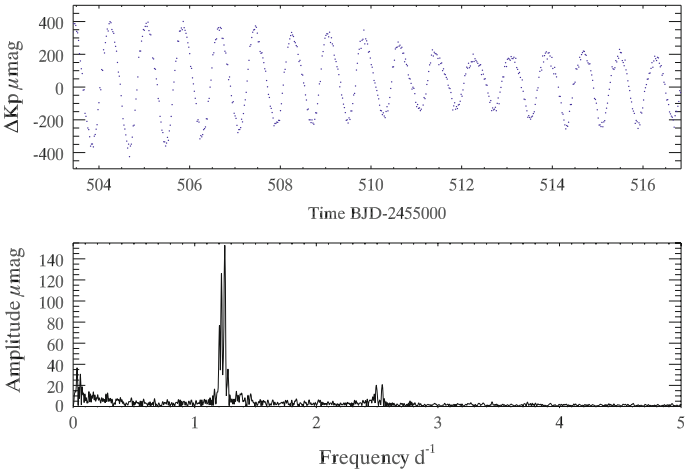

Fig. 2.10 *Lower panel* example of the low-frequency peaks seen in the Fourier transform, with a segment of the corresponding light curve (*upper panel*). Example given is KIC 11443271, LC, Q7 PDC-MAP data

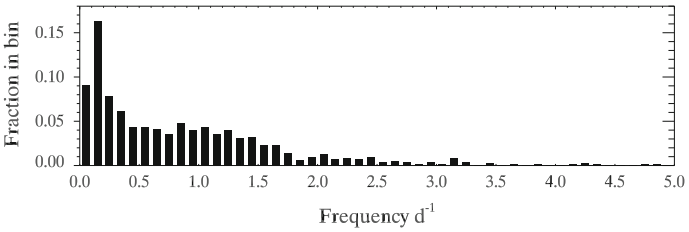

Fig. 2.11 Histogram of the frequencies of the Fourier peaks, for stars satisfying 7,000 $\leq$ KIC $T_{\rm eff} \leq$ 10,000 K. Break-up velocity for a 2-$R_\odot$ star occurs at $\sim$4 d^{-1}

low frequency is due to rotation, the distribution of low frequencies (Fig. 2.11) can be matched with A-star rotational distributions from the literature.

To this end, I prepared an observing proposal to obtain spectra for a sample of A stars that did not pulsate, in order to remove the influence of combination frequencies (combination frequencies are discussed in detail in Chap. 4, but for now can be considered a property or consequence of pulsation). This has the added benefit of obtaining spectra for stars that are likely, through their lack of pulsation, to be chemically peculiar. This particular idea is developed in the next chapter. Although only a fraction of the target list was observed due to bad weather, the obtained spectra were supplemented with ground based observations of suitable resolution and wavelength coverage that were originally taken for other purposes. If the spectroscopic and Fourier-inferred rotational velocity distributions agree, the low frequency variations could offer a constraint on the inclination angle for individual stars, or give an

indication of the equatorial rotational velocity without the need for time-consuming ground-based follow-up. In particular, if the Fourier transform peak corresponds to a rotation frequency, then a suitable radius estimate should, of course, yield a value of $v_{\rm rot}$ that is greater than the measured $v \sin i$ for every single star that can be measured, except, perhaps, for some unlikely combinations of latitudinal differential rotation and inclination.

Before the analysis could be completed, Balona, a co-investigator in the project, proceeded with the Fourier analysis independently, publishing the results in a single-author paper (Balona 2013). While the spectroscopic analysis remains as future work, the present discussion focuses on Balona's study. The frequency distribution he found is a match to that shown here in Fig. 2.11, and Balona showed this to match the rotational velocity distribution of A stars in the literature, specifically that of the Glebocki et al. (2000) catalogue.

In Balona's paper, the physical mechanism most strongly proposed for the production of the observed light variation is spots, and specifically spots that are akin to those seen in cooler stars. Surface magnetic fields can be generated at the base of the convective envelopes of cool stars, and these fields lead to the production of spots of cooler temperature that cause a reduction in observed intensity when they are on the observed hemisphere. The scientific interest in Balona's paper is that such spots are not expected in A stars, whose surface convection is inefficient at late-A and nearly absent for stars earlier than this. Without the surface convection, how can spotted-star signatures be generated in the light curve? There are actually many ways to achieve this, although the presence of spots intrinsic to a single A star, that result from activity (i.e. they are not Ap spots), is yet to be demonstrated as one of them.

In his Fig. 3, Balona (2013) presents some examples of periodograms of hot A stars, with the implication that the frequencies below $\sim$2.5 d^{-1} that are therein illustrated arise from spots on the rotating surface. KIC temperatures are well known to be underestimated for stars hotter than around F0, so selecting a $T_{\rm eff}$ range up to 10,000 K results in some of the 'A stars' presented being B stars, further eliciting an explanation of a physical mechanism capable of generating spots in such hot stars. It turns out that for the 'spotted' stars that were checked for this discussion, other mechanisms are viable: ellipsoidal variables are capable of producing Fourier transforms like these, though detailed fitting is still required. Some of Balona's spotted stars were clearly slowly pulsating B (SPB) stars, whose instability strip lies at late-B. A background giant could easily contaminate the light curve and generate a similar signal, too, because the amplitudes of the peaks are often small fractions of a mmag, but again detailed testing is required. Modelling light curves of late-B stars with spots has been attempted, but with limited success (Degroote et al. 2011), and a physical mechanism for the production of spots that fit the observations is still lacking.

Spots in cool stars migrate to different latitudes and change size, and there are usually multiple spots on any given hemisphere at any given time (except, perhaps, at the minimum of the activity cycle). This leads to phased light curves that change with time, unlike those of Ap stars (discussed in Sect. 2.3), whose spots are not free to migrate, and of ellipsoidal variables. The Fourier transform, in turn, shows a broader

peak or set of unresolved peaks in the former case, but sharp peaks in the latter cases. Harmonics may also be present if there is some variability happening multiple times per cycle, such as antipodal Ap spots that are both observable at different rotation phase, or an elongated hemisphere of an ellipsoidal variable that is visible twice per orbit. In these ways, one might distinguish the spots that Balona proposes from those of Ap stars or from ellipsoidal variables, but he does not attempt such a distinction; it is shown that the amplitudes of the low frequencies are significantly variable in some cases, though. Even if a phased light curve shows temporal evolution, it must be demonstrated that the spots are on the A star, and not a contaminant. Although KIC contamination is not reliable at small ($\lesssim$0.01) values, at large values one cannot ignore contamination. Balona made no rejection of contaminated objects, yet a check of some of his example stars shows objects with contamination exceeding a few tenths.

In conclusion, it may be possible to infer rotational velocities from Fourier transforms, but that this is generated by spots akin to those in cool stars as Balona (2013) suggests is yet to be demonstrated, and a substantial fraction of his 'spotted' stars can be shown to be binaries, pulsators or contaminated objects.

2.3 The Magnetic Ap Stars

The frequency of Ap stars among field stars peaks at 13 % at about B9 (Wolff 1983), where the distribution of the cooler Ap SrCrEu stars overlaps with that of the hotter Ap Si stars. Spectral classification tends to lead to later types being assigned than would be inferred from the photometric classification ($B - V$). Since many of these objects are actually B stars, the class is sometimes called "the ApBp stars", though cool Ap stars are even found at early-F.

The field strengths in magnetic Ap stars typically range from 0.3 to 30 kG (Braithwaite et al. 2010), and are responsible for most of the observed peculiarities in these objects, either indirectly, by reducing the rotation speeds of these stars to values low enough that meridional circulation no longer efficiently mixes the chemical composition, as we shall see in Sect. 2.3.2, or directly by concentrating certain elements into anomalous abundance patches on the surface.

2.3.1 The Oblique Rotator Model

The Rigid or Oblique Rotator Model (originally proposed and dismissed by Babcock in 1949, developed in a time-series photometric, spectroscopic and polarimetric case study by Stibbs (1950), yet more often attributed to Deutsch 1956) describes a rigid rotator—one with no large-scale differential flows—whose observed magnetic field strength changes as the star rotates, providing the rotational axis is not along the line of sight. The magnetic field is inclined to (or *oblique* to) the rotational axis, and

plays a dominant role in stabilising against convective motions near the surface. This reduces mixing of material, and allows the segregation of elements through atomic diffusion (i.e. gravitational settling and radiative levitation). The magnetic field also concentrates rare-earth elements into anomalous abundance patches or 'spots' on the surface, whose photometric intensity and spectral line profiles differ from the surrounding photosphere. As the star rotates and these antipodal spots, located near or on the magnetic poles, move with respect to the line of sight, periodic changes are observed in the atmospheric properties, as illustrated in the aforementioned case study by Stibbs (1950). These variables are known as α^2 CVn stars. The apparently dipolar magnetic fields in these stars are strong, the strongest being Babcock's star (HD 215441; 67 kG) , whose geometry has been reviewed by Landstreet et al. (1989). Although the fields appear dipolar, Braithwaite (2008) showed that roughly axisymmetric, stable magnetic fields consisting of a poloidal and a toroidal component can take on a dipolar appearance, implying the fields can be strongly non-dipolar.

Moss (1990) performed simulations of the evolution of the angle between magnetic and rotational axes, χ, and found the angle to increase over $t_{\rm MS}$. North (1985) observed the distribution of χ to be apparently random on the ZAMS, but increasingly bimodal with time, depending on whether toroidal or poloidal magnetic fields are present. In both cases, it appears that the time-scale for χ drift is only slightly shorter than $t_{\rm MS}$, because the initial random distribution of χ is recoverable yet an increasing bimodality is observable. Wade (1997), too, found intermediate values of χ for stars as old as 10^9 yr, but Landstreet and Mathys (2000) found that the slowly rotating Ap stars (periods longer than a month) generally had magnetic and rotational axes aligned to within about 20°, whereas χ was much larger in the short-period Ap stars. Hubrig et al. (2007) investigated obliquity angles for stars either side of the $3.0\,{\rm M}_\odot$ boundary. They agreed that the slower rotators tend to have fields aligned or nearly aligned with the rotational axis, regardless of mass, but that otherwise the evolution of obliquity is different for high- and low-mass Ap stars. Landstreet and Mathys (2000) discussed many potential causes for the alignment of fields with the rotational axis in slow rotators, with some causes arising from rotational braking through magnetic processes (accretion, stellar wind) occurring in the pre-main sequence phase. This is the subject of the next section.

2.3.2 Pre-main Sequence Evolution

The seminal paper of Stępień (2000) covered the pre-main sequence evolution of Ap stars in some detail. The following discussion is derived mostly from Stępień (2000), with some smaller contributions from other works.

Stępień sought to explain the observational result that Ap stars are slow rotators in light of the fact that they appear not to be braked on the main sequence (Hartoog 1977; North 1984, 1985). He determined that of all the possible reasons for the slow rotation he presented, only one was testable and satisfies the observations: that they

emerge from the intense contraction phase of stellar formation with angular momenta similar to those of normal stars, but lose most of it in the pre-main sequence phase.

In the stellar interior, fossil magnetic fields are destroyed in convective zones (and replaced with dynamo fields) but can persist in stars with fully radiative envelopes on time-scales much longer than the $t_{\rm MS}$ of an intermediate-mass star. In stars more massive than about $1.5\,{\rm M}_{\odot}$, the fully convective contraction phase is probably too short ($<10^5$ yr) to destroy the fossil field. Ap magnetic fields had already been determined to be fossil fields from observational considerations of the uniform distribution of Ap stars across the main sequence (North 1993; North et al. 1997; Wade 1997). In addition, Leroy et al. (1994) supposed that a fossil field theory fits better than a dynamo one for the Ap stars because stars with similar field strengths are observed with periods ranging from 4 d to 77+ yr.

Three major factors are important in the braking of Ap stars in the pre-main sequence phase: torque exerted by the interaction with the disc, accretion from the disc onto the star, and a magnetised wind. Stępień found that only for weak magnetic fields does accretion dominate period changes in early phases of the pre-main sequence evolution. Later in the pre-main sequence evolution, disc locking becomes very important and is the limiting factor of any spin-down, allowing rotational periods to become several times longer than those of normal stars, but not longer than that. Indeed, it is disc locking that prevents most stars reaching rotational periods of years.

The role of the disc is complicated, in that it initially acts to spin up the star, but later acts to maintain a constant rotational velocity, and thus acts counter to spin-down mechanisms imposed by both the wind and the magnetic field. When stars possess both magnetic fields and accretion discs, they will accrete matter along magnetic field lines, and thus enhance their surface content of refractory elements.

Stępień examined the effect of switching off the disc early. Since the disc's early effect is to spin up the star, early switch-off in massive stars would produce magnetic stars with abnormally high rotational velocities because the pre-main sequence phase is fairly short, and there is insufficient time for other factors (wind, magnetic field) to spin the star down again. Conversely, lower-mass stars that spend longer in the pre-main sequence phase will have very long rotational periods when the wind and magnetic field operate without opposition from the disc.

The property to which angular momentum loss is most sensitive is the strength of the magnetic field, because it affects each spin-down mechanism. The field interacting with the disc itself produces a torque on the star, and any magnetised wind will also carry away stellar angular momentum. Stępień found that a threefold increase in magnetic field strength produces a 300-fold increase in ZAMS rotational period for a 1.5–$2.0\,{\rm M}_{\odot}$ star. Indeed, early disc switch-off has a substantially greater effect in these lower mass stars only if the field strength is high. It is these extreme circumstances that might produce Ap stars with periods on the order of a century. Such stars are more common than any of the rotational distributions presented in Sect. 2.2 predict, though this is likely contributed to by an observational selection effect (Mathys 2004) due to the systematic search for stars with magnetically resolved lines

(such as the search conducted by Mathys et al. in 1997) preferentially detecting very slow rotators.

Although the pre-main sequence braking works efficiently for magnetic Ap stars, it doesn't explain the slow velocities of metallic-lined (Am) stars or the non-magnetic Ap stars. The former are explained via tidal deceleration in binaries, which will be addressed in Sects. 2.4.2 and 2.4.3, but the latter remain unexplained.

2.3.3 Main Sequence Evolution

There is disagreement in the literature over the main-sequence evolution of Ap stars, mostly in terms of their distribution across the HR diagram. We mentioned in Sect. 2.3.2 that Ap stars had been observed with a uniform distribution across the main sequence (North 1993; North et al. 1997; Wade 1997). Similarly, North (1998) concluded that there is no indication of any loss of angular momentum on the main sequence for Ap Si stars, and Hubrig et al. (2000) found no correlation between Ap rotational periods and fraction of main-sequence lifetime completed, confirming Stępień's work showing the angular momentum evolution to happen in the pre-main sequence phase. Hubrig et al. (2000) looked for progenitors of Ap stars on the main sequence. They found no statistically significant difference between the $v \sin i$ of young and old A stars in the 1.7–2.5 $M_\odot$ range, but did find a marginally significant population of slow rotators among the young A stars. All of these finds argue against the evolution of Ap rotational velocities on the main sequence.

Hubrig et al. (2000), on the other hand, found that magnetic Ap stars with masses below 3 $M_\odot$ were concentrated towards the centre of the main-sequence band—they have completed 30 % of their main-sequence life before magnetic fields become detectable. Although Hubrig et al. found no evidence for magnetic braking on the main sequence, the observational results of this study appear questionable in light of other studies. For instance, if the Ap progenitor already rotates slowly before presenting an observable magnetic field, why is it not an Am star? Abt (2009) comprehensively addresses this question and concludes these normal slow rotators are the Ap SrCrEu stars yet to develop peculiarity. If a strong magnetic field is required for the pre-main sequence braking, then why does it disappear for the first 30 % of t_{MS}? Hubrig et al. (2000) suggested the magnetic field could be complicated, either disorganised or buried below the surface. Furthermore, it could be that the type of extreme abundances that attract observational surveys do not develop in the first 30 % of t_{MS}, but this is contrary to long-standing theoretical work that the stability generated by magnetic fields facilitates the establishment of chemical peculiarities within 10^6 yr (Michaud et al. 1976); some claim even in just days for Sr in the high atmosphere (Braithwaite et al. 2010). Ultimately, the search for Ap progenitors in general suffers from insufficient data: Hubrig et al. determined that an extension of their sample to ~2,200 stars would be required to generate a 3σ detection.

Kochukhov and Bagnulo (2006) re-opened the debate with public data for 150 CP stars with accurate *Hipparcos* parallaxes. They found the highest number density of

CP stars was in the 2.5–3.0 $M_\odot$ bin, and that at these masses the CP stars occupy the full width of the main-sequence band. At masses lower than this the CP stars are absent in the final tenth of t_{MS}, but there is no agreement with the findings of Hubrig et al. (2000) that no Ap stars are found younger than $t/t_{MS} = 0.3$. Later analyses found that Ap stars with $M \leq 3.0\,M_\odot$ were indeed clustered around the middle of the main-sequence band, but that Ap stars more massive than $3\,M_\odot$ occupy the full width of the main-sequence (Hubrig et al. 2006, 2007).

2.4 Binaries

The binary frequency of A stars lies at around 35 % (Abt 2009), and is not abnormally high. Table 2.1 shows the observed binary frequency for main-sequence stars. In this section we will discuss the effect of binarity on the rotation rates of the A stars.

2.4.1 Observational Results

Abt and Boonyarak (2004) collected orbital data for 400 stars of types B (162 stars) and A (238 stars). They found that "the amount of angular momentum lost, presumably by tidal effects, decreases with increasing binary separation and increases with stellar ages or types". Their study is significant in that they look not just at close binaries, but those whose orbital periods lie between 4 and 500 d such that they cover periods where synchronisation is not expected. In fact, the authors were surprised to observe tidal effects up to these long periods, given that for A stars, theoretical limits for circularisation and synchronisation were 1.58 and 0.95 d, respectively (Zahn 1984).

Table 2.1 Summary of observed spectroscopic binary frequencies for main-sequence stars

Type	Sample	Binaries found	Frequency (%)	Source
O	227	54	24 ± 3	Mason et al. (1998)
B2-B5	48	19	40 ± 9	Abt and Levy (1978)
A0-A9	119	41	35 ± 5	Abt (2009)
F7-G8	175	38	22 ± 3	Abt and Willmarth (2006)
M	64	8	13 ± 4	Marcy and Benitz (1989)

Table and caption from Abt (2009, Table 1). Permission obtained from author, and reproduced by permission of the AAS

The amount of angular momentum lost as a result of being in partially synchronised[2] binaries of types A6–F0 was found to range from 90 % at $P_{\rm orb} = 5.5$ d, to 40 % at $P_{\rm orb} = 100$ d. The authors added that no significant differences in losses were found for single-lined (SB1) or double-lined (SB2) binary systems, so these effects are not sensitive to the secondary masses. However, the results are purely observational and do not require that the braking occurs on the main sequence; they are open to interpretation and perhaps the spin-down occurs during formation.

At periods exceeding 500 d, the rotational velocities are a statistical match with single stars, i.e. no braking is observed, but A0–A5 binaries with periods of 4 d to 500 d rotate on average at 31 ± 2 % of single star velocities (the numbers for B-type and A6–F0 stars are 67 ± 5 and 41 ± 15 %, respectively).

Kogure (1981) looked at the period distribution of binary systems with A0–A9 V–III primaries (from various catalogues), for the purpose of deriving a period-rotational velocity relationship, and found the maximum of the period distribution to lie at $P_{\rm orb} \approx 5$ d. Kouwenhoven et al. (2005) observed 199 A and late-B members of the nearby Scorpius OB2 association in the near-infrared, though their method appears to have been sensitive to long periods only, covering ranges of several decades to several thousands of years, thus having the opposite period sensitivity to spectroscopic surveys. No period distribution could therefore be inferred. However, among their results they found that the mass ratio, q, of secondary to primary covers the whole range from 0.1 to 1 for primaries between 1.5 and 2 $M_\odot$, and from 0.1 to 0.75 for 2–3 $M_\odot$ stars. The normalised mass-ratio distribution, $f(q)$, is described empirically as $f(q) = q^{-0.33}$, and is important in braking calculations (cf. Sect. 2.4.2). They also found a lower limit to the multiplicity (*not* duplicity) of A stars of 0.4, in agreement to that of Abt (2009) once one accounts for the duplicity/multiplicity difference.

To obtain larger-number and complete statistics on the short-period binary distribution, Mazeh et al. (2006) constructed a 938-star subsample of eclipsing binaries with main sequence B-type primaries from OGLE photometric data of the LMC in an automated way. They find a "somewhat surprising" flat distribution in $\log P$ between 2 and 10 d (Fig. 2.12), after trimming their sample to improve homogeneity and correcting for detection probability. As such, although their results are based on the eclipsing binaries, the corrections applied in the lower panel of Fig. 2.12 extend its applicability to all LMC binaries, not just eclipsing ones. One cannot just extend the distribution to A stars, but at least for the early-A stars, it is hard to see that the distribution would change drastically.

2.4.2 Short-Range Tidal Braking

Working on the idea that the dominant non-adiabatic damping mechanism operating in stars with convective envelopes is turbulent friction, Zahn (1977) derived an

[2] The meaning of 'partially synchronised' is not explicit in that paper. It sometimes means stars that are synchronised at periastron, when orbits are highly eccentric, but in this case perhaps means stars that show some tidal braking but are not fully synchronised.

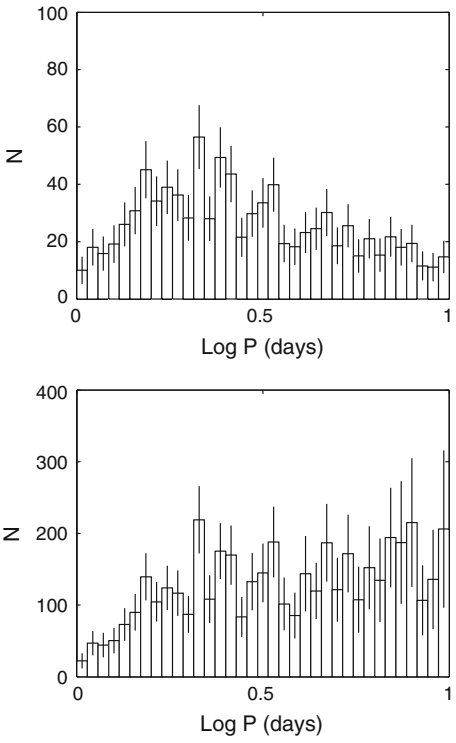

Fig. 2.12 *Top panel* raw period distribution of the bias-free sample. *Bottom panel* period distribution corrected for the detection probability. Figure and caption from Mazeh et al. (2006, Fig. 1). Permission obtained from Astrophys. Space Sci. (Springer)

expression for the time-scale of synchronisation, $t_{\rm syn}$, of low-mass (i.e. convective envelope) main-sequence binaries: $t_{\rm syn} \sim q^{-2}(d/R)^6$, where d is the orbital separation and R the radius of the star to be synchronised (Langer 2009). The stars with radiative envelopes, however, are damped radiatively by tidally induced gravity-mode pulsations on time-scales of $t_{\rm syn} \sim q^{-2}(1+q)^{-5/6}(d/R)^{17/2}$ (Zahn 1975). We are concerned here with the latter time-scale.

The time-scale increases rapidly with decreasing q, the process being twice as efficient for $q = 1$ as $q = 0.75$, but the most important parameter is the binary separation, d/R, here expressed in stellar radii, for which the exponent is high. The mechanism decreases extremely quickly in efficiency for greater separation, and is only effective at ranges closer than $\sim d/R = 6$, corresponding to a physical separation of <0.07 AU ($P_{\rm orb} < 2.5$ d) for a $2.5\,{\rm R}_\odot$ primary.

2.4.3 Medium-Range Tidal Braking

The short-range mechanism accredited to Zahn is not the full story in tidal braking. The theoretical limits calculated by Abt and Boonyarak (2004) based on Zahn (1984),

for circularisation and synchronisation periods of 1.58 and 0.95 d, respectively, do not perfectly match the observations. Abt et al. (2002) observed values of 4.9 and 2.5 d instead, and found rotational velocities reduced, but not synchronised, for up to twice these periods. In Sect. 2.4.1 we pointed out the severe braking observed by Abt and Boonyarak (2004) for periods up to 500 d. Some other mechanism would appear to be braking these stars effectively at much larger distances than Zahn's.

Tassoul and Tassoul (1992b) presented such a mechanism. So-called 'Ekman pumping' is a mass-transfer process (hence transporting angular momentum) between the surface and the inviscid interior. It allows effective synchronisation within a time much shorter than $t_{\rm MS}$ by redistributing angular momentum within the star. Large-scale meridional flows are set up from equator to pole at the surface, but from pole to equator in the interior. The equatorial material of high angular momentum is thus regularly replaced with lower-angular momentum material from the interior, and the star is spun-down exponentially in the rotating frame. Rieutord (1992) made calculations refuting the Ekman-pumping mechanism, but the Tassouls showed Rieutord's calculations to have omitted tidally driven currents, inappropriately assumed solid-body rotation, and to have failed to incorporate tidal lag.

Tassoul and Tassoul (1992a) explained their mechanism in a way that is more easily accessible to the general reader: the presence of a binary companion elongates the primary along the line connecting the two. A particle rotating around an axis perpendicular to this line thus travels in an ellipse, rather than a circle, and accelerates and decelerates along its path. Large-scale meridional flow thus comes into existence in a non-synchronous binary component. The resulting replacement of high angular velocity fluid with low angular velocity fluid is more efficient than viscous friction, spinning the star down efficiently. The synchronisation time can be calculated as follows:

$$t_{\rm syn}({\rm year}) = \frac{14.4 \times 10^{-N/4}}{q(1+q)^{3/8}} \left(\frac{\rm L_\odot}{L}\right)^{1/4} \left(\frac{\rm M_\odot}{M}\right)^{1/8} \left(\frac{R}{\rm R_\odot}\right)^{9/8} \left(\frac{d}{R}\right)^{33/8}$$

where the constant factor 10^N is the ratio of the macroscopic and microscopic viscosities (typically $N = 0$ for radiative envelopes and $N = 10$ for convective ones).

Tassoul and Tassoul (1992a) compared their theory with Zahn's. While Zahn's mechanism has dependencies of $(d/R)^6$ for a convective envelope and $(d/R)^{8.5}$ for a radiative one, the Ekman-pumping mechanism has a dependency of $(d/R)^{4.125}$. The latter is therefore effective at longer ranges than the other two, being effective up to $(d/R) \sim 20$ rather than $(d/R) \sim 6$. It can remain operative up to $\sim$100-d periods for early-type stars without causing full synchronisation beyond $P_{\rm orb} = 15$–25 d. It is thus compatible with the observations described in Sect. 2.4.1.

Some qualifications are applicable to the Tassouls' mechanism. Their equations require the stellar radius to be constant over the braking time-scale. For longer periods, this time-scale is longer and the validity breaks down because some radius evolution occurs. An expanding radius affects conservation of specific angular momentum and acts against synchronisation. Furthermore, moderately small eccentricities were

assumed, so that just like Zahn's (1977) mechanism, the assumptions are invalid for moderate or high eccentricities. (One must realise, of course, that for high eccentricity pseudo-synchronous rotation is all that is possible.)

Witte and Savonije (2001) developed another medium-range mechanism that works specifically on eccentric binaries. It works when an orbital harmonic becomes locked on a resonance, is sustained in that resonance state for a prolonged time, and affects the spin and orbit significantly in that time. The harmonic remains locked in resonance, exciting gravity-mode oscillations, until either the power redistribution in the orbital harmonics becomes too large or some other frequency comes into resonance and pushes the other one out (cf. heartbeat stars, Thompson et al. 2012). Witte and Savonije find that for a simulated 10-d orbit of two $10\,M_\odot$ stars, the accumulated time during which at least one star is locked in resonance spans 64 % of the total evolution time, while 81 % of the total eccentricity decrease is accounted for during the locking periods: the total decrease in this case being from $e = 0.6$ to 0.2 in just a few Myr.

With a period of 20 d, i.e. doubled from the previous simulation, the efficacy of locking at reducing the eccentricity is quartered, but still important. Although in the first 4 Myr $P_{\rm orb}$ drops by a quarter and eccentricity by a fifth (from 0.60), the rotation rates do not decrease over this time and 4 Myr is roughly one eighth of the main-sequence lifetime for a $10\,M_\odot$ star.

However, we are concerned with stars of lower mass than this. How might the results change for a $2.0\,M_\odot$ star? Witte and Savonije do not comment on this, but intuitively it seems that the braking mechanism would become less effective with a lower-mass primary. We must also consider, though, that the main-sequence lifetime of a $2.0\,M_\odot$ star is far longer than that of a $10\,M_\odot$ star, so the mechanism can act for much longer. Hence if time is measured in fractional main-sequence lifetime, then there is little reason to suspect the mechanism would not work for lower-mass stars. No comment was provided on the effect of decreasing q, either. It would certainly serve to decrease the efficiency, but it is not known by how much.

The orbital harmonic locking mechanism is much more efficient for higher eccentricities, and, although it doesn't brake rotational velocities greatly, it has a large effect on the orbital period. As such that may bring the stars close enough and begin to circularise the orbits so that Zahn's short-range mechanism or the Ekman-pumping mechanisms can reduce the spin to observed levels. We will take a closer (simple) look at angular momentum transfer in binary orbits in Appendix B of this chapter, but a full-scale theoretical investigation is beyond the scope of this work.

2.5 Metallic-Lined A Stars (Am Stars)

The classical Am stars are those whose Ca II K line types appear too early for their hydrogen line types, and metallic-line types appear too late, such that the spectral types inferred from the Ca II K and metal lines differ by five or more spectral subclasses. They are observed to be slow rotators with $v \sin i < 120\,\mathrm{km\,s^{-1}}$, and

although some Am stars are observed with higher rotational velocities, there is a strong observed correlation between slow rotation and abundance anomalies, and the standard Am-star model requires it. This section pertains specifically to the rotational velocity properties of Am stars, and their presence in binary systems. More details on the line strength anomalies and the peculiar abundance model are given in Chap. 3.

2.5.1 Presence in Binaries

The slow rotation of the Am stars is largely brought about by their presence in short-period (1 d $\leq P \leq$ 10 d) binary systems (Abt 1967). The exact fraction of Am stars in binaries is not certain. Historically, the number was believed to be high—Abt (1961) measured 22 of 25 (=88 %) stars in his survey to be binaries, and Vauclair (1976) put the number at about 80 %—but more recent surveys with less observational bias put the percentage between about 60 (North et al. 1998) and 54 (Debernardi 2000). In another study (Debernardi et al. 2000), the binarity of 19 Am stars in the Praesepe and Hyades clusters was established to have a lower limit of 63 %, and the authors could not definitively rule out that the percentage of single Am stars might be zero. This binary frequency is to be compared to the much lower value of 35 % of A stars as a whole (Abt 2009, cf. Table 2.1 here). It is the tidal interaction in close binaries that brakes the stars' rotational velocities, with different mechanisms being dominant at different stellar separations (Sects. 2.4.2 and 2.4.3).

Since Am stars require slow rotation to facilitate gravitational settling and radiative diffusion (e.g. Baglin et al. 1973) , those Am stars that are not in binaries and thus not tidally braked require an explanation for their slow rotation—how do single Am stars come to possess such small rotational velocities? The majority of A stars have rotational velocities higher than the observed upper limit of Am star velocities, but could the single Am stars simply lie at the lower end of a normal distribution of rotational velocities, low enough to fall below the observed Am star rotational velocity limit and thus require no braking? Arguments presented in Sect. 2.2.1 suggest the distribution is multimodal, and that the population of Am and Ap stars belong to their own Maxwellian, not the same as the normal stars. In Sect. 2.3.2 it was found that pre-main sequence braking is extremely efficient when a star possesses a magnetic field, but that some slow rotators emerge from the pre-main sequence phase without strong magnetic fields, and that the fields are perhaps buried. Maybe these stars can become single Am stars?

The 'single Am' problem remains an unsolved one. One of the greatest difficulties lies in eliminating the presence of a companion for a large sample of 'single' Am stars.[3] Abt (1979) presented a different hypothesis based on a study of Am stars in clusters. While he did find Am stars in the youngest cluster, implying the Am star

[3] Unlike our Solar System, where Jupiter contains most of the angular momentum, A stars rotate so rapidly that a planet of Jupiter's mass and orbital parameters would contain on the order of 1 % of

spectral peculiarities develop in less than 10^6 y (after the suggested age correction of Abt 2009 is applied), he found that in the youngest clusters the Am stars have $v \sin i$ far greater than the observed limit of field stars of $\sim 120\,\mathrm{km\,s^{-1}}$. Though this has never been confirmed, it would mean the Am stars do not have to be slowly rotating, but perhaps that in most cases the mechanism causing the spectral peculiarities also causes the slow rotation. The hypothesis is interesting, and Abt derived an empirical rotational braking relation: $\langle v \sin i \rangle \propto T^{-0.28}$, where T is the cluster age in years, but Am star theory requires slow rotation and the post-peculiarity braking hypothesis finds little mention in the literature. The consensus is that that study was based on too few data points (e.g. Stępień 2000).

2.5.2 *Implications on Mixing*

The various mechanisms for tidal braking in Sect. 2.4 each impose large amounts of mixing of material in the stars concerned. The Witte and Savonije (2001) method, involving orbital harmonics in resonance with g modes, sees the low-order orbital harmonics grow to high amplitudes during resonance crossings, and "these crossings could possibly induce large-scale mixing". Similarly, the meridional circulation set up during Ekman-pumping (Tassoul and Tassoul 1992a, b) will also thoroughly mix material. Zahn's 'turbulent friction' mechanism (Zahn 1975, 1977), involves coupling between convective motions and tidal oscillations (at least, it does in reality—it was not realistically treated in the initial derivation). Thus all three tidal braking mechanisms act to mix the stellar material, contrary to observations that Am stars are vertically stratified in elemental abundances, and are largely found in close binaries. Perhaps it is the case that the mixing halts once the stars attain synchronisation, but this would be testable in that no Am star should be observed outside of synchronisation—we have just seen that this is not the case, and Murphy et al. (2012) have recently presented a case-study of an intriguing single Am star observed by *Kepler*, KIC 3429637. This will be presented in Chap. 5. Further discussion of those mixing processes not induced by binarity will be discussed in Chap. 3.

2.6 The Kraft Break

The A stars rotate much more quickly than the late-F and G stars. Even many of the slowly rotating A stars are not slow by comparison with the average G-dwarf; the normal A stars rotate faster than those by an order of magnitude or more. The two regimes have their 'transition' at around spectral type F5 V, that is, normal stars earlier

(Footnote 3 continued)
the angular momentum of the star, thus distribution of angular momentum into planetary systems is not a viable mechanism for achieving a slowly rotating single A star.

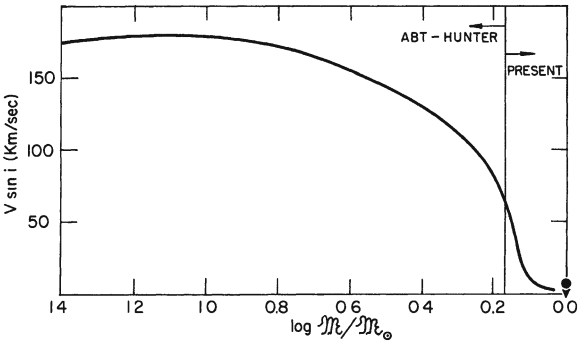

Fig. 2.13 $\langle v \sin i \rangle$ as a function of $\log M/\mathrm{M}_\odot$ for field stars. The masses were determined from the work of Abt and Hunter (1962) and Kraft's $v \sin i$ values were adopted. The greatest rate of change of $v \sin i$ with mass occurs for $\log M/\mathrm{M}_\odot = 0.13$ ($M = 1.35\,\mathrm{M}_\odot$) corresponding to spectral type ~F5 V. Figure from Kraft (1967, Fig. 2). Permission obtained from author, and reproduced by permission of the AAS

than about F5 rotate quickly and those later than F5 rotate slowly. This boundary is known as the Kraft break, after Robert Kraft who first explained the phenomenon (Kraft 1967).

From observations of over 200 field stars, Kraft showed that a break in rotational velocities of over an order of magnitude occurs over a very small mass range. The mean $v \sin i$ of $1.3\,\mathrm{M}_\odot$ stars lies at around $20\,\mathrm{km\,s^{-1}}$, compared to $\sim 75\,\mathrm{km\,s^{-1}}$ for a $1.6\,\mathrm{M}_\odot$ star, as shown in Fig. 2.13.

To be specific, this relationship of $v \sin i$ with mass was found for stars without chromospheric Ca II K line emission, which is an important indicator of age and activity in the late-F and G stars—Ca II K line emission is seen in the younger stars with more active convection zones. The average rotational velocity was seen to be higher in stars with Ca II K line emission than without. Kraft's results thus show that young stars are braked by magnetic winds coupled to the surface hydrogen convection zone, such that once they reach an age where the stellar activity has lessened, they have been strongly braked. Stars of later spectral types will have spent more time on their Hyashi tracks in a fully convective state, and thus reach the ZAMS having been braked substantially more. The braking rate depends on both the convection zone overturn time-scale and the depth of that convection zone (see Sills et al. 2000 for a well-referenced introductory review). Early-F stars do not have a deep Hydrogen convection zone on the main sequence, and so are not braked by magnetically coupled winds after reaching the ZAMS.

Irwin and Bouvier (2009) emphasize the importance of the circumstellar disc on the pre-main sequence in regulating the rotational period. We saw this argument earlier from Stępień (2000) for the Ap stars. The duration of the pre-main sequence phase for which the disc is present depends on the stellar mass, in that the less massive stars spend longer in this phase and are influenced by the presence of the disc for longer. The disc acts to maintain the stellar rotational period at a constant value; in

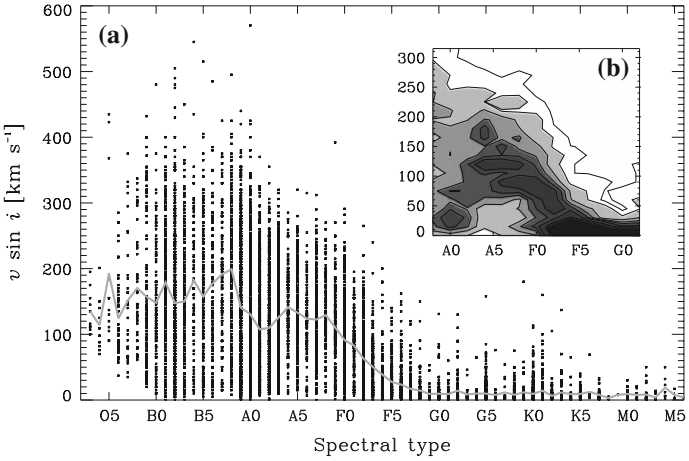

Fig. 2.14 **a** Distribution of $v \sin i$ as a function of spectral type. The individual values (*crosses*) represent individual stars. The variation of the average $v \sin i$ per spectral type (*solid thick line*) is also over-plotted. **b** The sub-panel in the upper-right corner represents the color-coded scale density of points in the same diagram $v \sin i$–spectral type; both axes have the same scale as in **a**. Darker tones stand for higher densities. The Kraft break is evident at ∼F5 as a high density of slow rotators and lack of fast rotators. The over-density of slow rotators at around A0 is the population of Ap stars. Figure and part of caption from Royer (2009, Fig. 1). Reproduced with kind permission of Springer Science and Business Media

the absence of the disc, the star would spin up as it contracts, meaning that the disc acts to slow rotation, whether it be through disc locking or accretion-driven stellar winds. This argument of pre-main sequence braking being strongly mass dependent furthers the conclusions of the model of braking through a magnetic wind during the main-sequence phase, and explains satisfactorily why the Kraft break is observed: the mechanisms that are more efficient on the pre-main sequence have less time to act in the more massive (earlier) F stars, so those stars leave this phase having been braked less, and they continue to be braked less on the main sequence because they have only shallow surface convection zones with which magnetic winds can couple. The complete picture of rotation versus spectral type is shown in Fig. 2.14.

2.7 Chapter Summary

We have seen that the distribution of rotational velocities in A stars ranges widely from essentially zero right up to $400\,\mathrm{km\,s^{-1}}$. The distribution cannot be represented empirically by a single Maxwellian; indeed, even two Maxwellians are insufficient because there exists separate populations of (i) normal, fast rotators; (ii) normal, slow rotators; and (iii) chemically peculiar (CP) slow rotators. CP fast rotators are generally not observed.

There is a discrepancy in $v \sin i$ determinations by different observers, with both systematic shifts and fractional differences. In particular, the results of Royer et al. (2007) are high compared to the literature values, especially those of Abt and Morrell (1995). The former authors' results are the most recent, and they had the opportunity to compare them to those of other groups. A comparison of two other sets of rotational velocities having stars in common with Abt and Morrell indicated the values of the latter are underestimated.

The evolution of rotational velocities among A stars is dissimilar to that observed for cooler stars. Only the late-A stars see substantial braking whilst approaching the TAMS. Intermediate A stars appear to brake little in the latter half of the time spent on the main sequence ($t_{\rm MS}$), but more massive stars are braked quite efficiently after $t/t_{\rm MS} = 1/3$.

All stars between 2 and $3\,{\rm M}_\odot$ are observed to *accelerate* while $t/t_{\rm MS} < 1/3$. This is explained as angular momentum distribution outward from a core that rotates faster on the ZAMS than the surface does. A reinvestigation of older studies, namely those of Slettebak (1955), Wolff and Simon (1997), and Erspamer and North (2003), has been performed here and shows agreement with the findings of Zorec and Royer (2012).

It may be possible to infer rotation frequencies from the Fourier transform of the light curve. Work to investigate this link, whose origin is unclear, is ongoing. Balona (2013) interprets the evidence as the presence of spots on the surface of 40 % of A stars and some B stars, but an analysis of several of his candidates for spots showed that binarity, pulsation or contamination were equally satisfactory matches to the observations, and require no new physics.

We examined the cause of slow rotation in Ap stars. Magnetic field strength is the main factor determining the extent of braking in the pre-main sequence phase, with the disc lifetime also playing an important role. The observed Ap star periods can be explained through pre-main sequence braking and, for the extremely slow rotators, with an additional observational selection bias. No unambiguous evidence for main-sequence braking of Ap stars has been presented, though the development time-scale for some spectral peculiarities can give the appearance of Ap stars lying only in the central third (measured from ZAMS to TAMS) of the main-sequence band. A 3-σ identification of Ap progenitors requires a larger sample than has currently been obtained.

We discussed the distribution of binary periods, which was recently observed to be approximately flat in $\log P_{\rm orb}$ for orbital periods between 2 and 10 d. Mass ratios appear to be able to take on a wide range at mid-A, with an empirical dependency $f(q) = q^{-0.33}$. At periods exceeding 500 d, rotational velocities resemble those of single stars. Between 4 and 500 d, increasingly-long orbital periods see decreasing amounts of braking. Below 4 d, orbits are observed to be fully synchronised.

Three mechanisms were presented for tidal braking: (I) The 'orbital harmonic resonances' mechanism works by locking orbital harmonics in resonances, during which they greatly reduce the eccentricity and period of the orbit. Resonances can account for over 50 % of the total evolution time. This mechanism does not slow the rotation but can reduce the orbit to a range where the other two mechanisms are

efficient. (II) The 'Ekman-pumping' mechanism operates with large-scale motions acting to replace high angular momentum material at the surface with lower angular momentum material from the interior. This is more effective than simple viscous friction, and efficiently brakes the stars within ranges of up to $\frac{d}{R} \sim 20$, i.e. separations up to 20 times the primary star's radius. (III) Zahn's 'turbulent friction' mechanism is very efficient but requires separations below $\frac{d}{R} = 6$.

Each of the mechanisms proposed for tidal braking would appear to mix the material too much to be compatible with Am star observations. Nevertheless, we reviewed the frequency of Am stars that are in binaries, the most recent estimates being on the order 55–65 %. It is very difficult to definitively rule out a companion from systems that appear to be single, so the binary fraction could be substantially higher than this.

The A and early-F stars rotate much more quickly than late-F and G stars. The Kraft break, occurring roughly at spectral type F5 V (corresponding to $\sim$1.3 $M_\odot$ stars) delimits the regimes of fast rotation in hotter stars, and slow rotation in cooler stars. The causes are differences in the duration of the pre-main sequence phase, during which deceleration is efficient, and the presence of deep hydrogen convection zones in the cooler stars, which facilitate braking on the main sequence though magnetic winds coupled to the convection zones.

Acknowledgments SJM would like to thank Antonio García Hernández and especially Don Kurtz for their useful comments, and Richard Gray for the discussion on spectral type calibrations. Appendix A to this chapter made extensive use of the SIMBAD database and the VizieR catalogue access tool (Ochsenbein et al. 2000), operated at CDS, Strasbourg, France.

Appendix A: Spectral Type Calibrations

In astronomy there are many different photometric systems in use, each with different filters. Systems come into and fall out of use over time; the nature of high-precision, ground-based, V-band photometry in the latter half of the previous century saw the narrow-band Strömgren filters become widely used. Now, many surveys in the infrared and ultraviolet favour broader filters, and all-sky surveys are adopting the Sloan system. Sloan may be the future, but much archived data exists in older formats that have seen more extensive calibration in the literature. It is these systems for which literature calibrations are assembled in Table A.1 in this appendix for reference. Calibrations of the main sequence under the Sloan system would be highly valuable but are yet to be performed, and so are not provided here.

The photometric parameters in Table A.1 are useful in many ways. The Balmer discontinuity parameter, $c_1 = (u - v) - (v - b)$, is an indicator of luminosity; $m_1 = (v-b)-(b-y)$ is the line-blanketing parameter, an indicator of metallicity; β is a narrow-band index measuring the Hβ line strength, mostly free from line blanketing and interstellar extinction, an indicator of temperature for stars between A3 and F2 (Joshi et al. 2006), and mildly sensitive to gravity due to pressure broadening of

Table A.1 Calibrations from the literature of spectral type, absolute visual magnitude M_V, colour $(B-V)$, and effective temperature for the stars around spectral type A at luminosity class V

Spectral type	M_V (mag)	$B-V$ (mag)	$T_{\rm eff}$ (K)	β (mag)	$(b-y)_0$ (mag)	m_0 (mag)	c_0 (mag)
B8	0.0	−0.11	12,000	2.748		0.118	0.66
B8.5	0.4	−0.09	11,600	2.772		0.122	0.75
B9	0.7	−0.07	11,200	2.795		0.126	0.83
B9.5	1.0	−0.04	10,650	2.827		0.134	0.97
A0	1.4	−0.01	10,150	2.861		0.154	1.01
A1	1.6	0.02	9,750	2.873		0.162	1.05
A2	1.9	0.05	9,300	2.885	0.029	0.169	1.08
A3	2.0	0.08	8,950	2.871	0.055	0.172	1.08
A4		0.12	8,500	2.864	0.071	0.184	1.05
A5	2.1	0.15	8,200	2.841	0.090	0.195	0.96
A6	2.2	0.17	8,000	2.833	0.099	0.198	0.93
A7	2.3	0.20	7,800	2.824	0.107	0.201	0.90
A8	2.4	0.27	7,300	2.789	0.132	0.194	0.87
A9	2.5	0.30	7,150	2.779	0.145	0.193	0.83
F0	2.6	0.32	7,000	2.768	0.158	0.191	0.79
F1	2.8	0.34	6,950	2.736	0.204		
F2	3.0	0.35	6,900	2.704	0.250		
F3	3.1	0.41	6,650	2.690	0.263		
F4	3.3	0.42	6,600	2.674	0.277		
F5	3.4	0.45	6,500	2.665	0.290		

Data taken from Gray and Corbally (2009) for M_V calibration against spectral type; from Fitzgerald (1970), who provides UBV data for many spectral types; and Bessell (1979), who provides calibrations of $T_{\rm eff}$ against $B-V$. The latter were fitted with a cubic polynomial, and $T_{\rm eff}$ was calculated for each $B-V$ quoted in the table, before being rounded to the nearest 50 K. Values of β and the de-reddened indices $(b-y)_0$, m_0 and c_0 are taken from Crawford's (1975, 1978, 1979) 'standard relations' that specifically correspond to the ZAMS, and their definitions are explained in this appendix; a few values had to be interpolated

the line. Smalley and Dworetsky (1995) calculated synthetic β values for a grid of $T_{\rm eff}$ and $\log g$ in their table 7. Another temperature indicator is $b-y$, which is "reasonably free of effects of [line] blanketing" (Crawford 1975), but is affected by reddening. The $B-V$ index is calibrated so that A0 stars have $B-V\equiv 0$, but the values in Table A.1 remain true to source.

Two indices from these values are commonly used to diagnose chemical peculiarity: $\delta m_1 = m_1({\rm standard}) - m_1({\rm observed})$, for a given β; and δc_1, rather confusingly defined in the opposite sense from δm_1 (the poor observer!), as $\delta c_1 = c_1({\rm observed}) - c_1({\rm standard})$, again for a given β. The standard relations can be found in Crawford (1975, 1978, 1979) for the F, B and A stars, respectively. A more negative δm_1 index indicates a stronger metallicity, and is typical in Am stars. A very small

($\lesssim$0.1) or negative δc_1 index is also seen in most Am stars, but not exclusively—both peculiar stars and binaries have small or negative δc_1 indices. Am stars have a smaller δc_1 index because of line blanketing, which describes the effect of metal lines on the spectrum and, due to the increase in density of spectral lines at bluer wavelengths, removes more flux at shorter wavelengths than longer ones. Since Am stars have stronger metal lines, line blanketing is greater, and the spectrum is reddened, causing δc_1 to decrease. Hence the trend noticed by Crawford (1979) that stars with larger negative δm_1 have smaller than average δc_1.

Occasionally the indices $(b-y)_0$, c_0 and m_0 appear in the literature, and are used in Table A.1. They indicate $(b-y)$, c_1 and m_1 values that have been corrected for reddening (Crawford 1975). $(B-V)_0$ is also occasionally seen, and a 'colour excess', defined as $E(B-V) = (B-V)_0 - (B-V)$ is commonly used to describe interstellar reddening. It is noteworthy that reddening for *Kepler* targets is negligible (Molenda-Żakowicz J. et al. 2009).

Literature values of M_V versus spectral type are not particularly consistent. A large difference is found by Gray and Corbally (2009) and Adelman (2004) for the early-A stars, for instance. Calibrations are frequently borrowed from various sources in a hard-to-trace way. For this reason I have calculated a new calibration for luminosity class V objects, using the Tycho-2 Spectral Type Catalog (Wright et al. 2003) and *Hipparcos* parallaxes. Existing calibrations of M_V with *Hipparcos* data against spectral type include that of Jaschek and Gomez (1998), unknown to this author at the time of the investigation with Tycho-2 data, where the luminosity class was the primary subject of investigation rather than the temperature subclass of the spectral type. Jaschek and Gomez used only MK standards, which when filtering out stars without parallaxes or with large errors, left them with only 96 stars in the range B0–F5. We shall see here that the Tycho-2 data have afforded numbers superior by two orders of magnitude.[4]

The Tycho-2 Spectral Type Catalog contains over 350,000 stars with spectral types. The positional matching of these stars is described as 'stringent', with 97.5 % of the stars being matched to within $1''$ of star positions from other cross-referenced catalogues. The catalogue also provides B and V magnitudes. The V magnitudes were used here with *Hipparcos* parallaxes to determine absolute magnitudes, and to calibrate these against spectral type. A calibration in $B-V$ has not yet been performed but is a possible direction for future work.

About half of the stars in the Tycho-2 catalogue do not have both spectral types and luminosity classes. Many more are not of spectral types B8–F5, and so were not of interest to the current study. Chemically peculiar stars were excluded, and any objects with two spectral types given (whether arising from uncertainty, binarity or some other source) were also rejected in the interest of creating a calibration for normal, single, luminosity-class V objects. These selection criteria reduced the initial 350,000 stars to about 35,000. A further requirement was that stars used must be

[4] The main conclusion of Jaschek and Gomez (1998), incidentally, was that the MK standards ought to be revised to eliminate the stars deviating furthest from a direct relation between luminosity class and M_V.

given the object type '$*$' in the Simbad database, further eliminating known binaries or multiple systems, peculiar stars other than the common Am or Ap types, and importantly, known variable stars. Finally, not all stars in the Tycho-2 catalogue have *Hipparcos* parallaxes available; those stars without parallaxes, or whose parallaxes were below 3 mas were rejected, since the errors on individual parallax measurements are on the order 1 mas. The final number of usable stars was 8,722.

Although Simbad offers other sources for spectral type and V, the values used were strictly the Tycho-2 values. This has two main benefits: (1) the spectral type sources are few in number (a result of the aforementioned selection criteria was that only three sources within the catalog were used: the catalogues of Jaschek et al. (1964) and Kennedy (1983), and all five volumes of The Michigan Catalog (Houk and Cowley 1975; Houk 1978, 1982; Houk and Smith-Moore 1988; Houk and Swift 1999), thus spectral types are internally consistent. (2) The Tycho-2 V values are given to a higher precision than most of the Simbad values, and have just one source.

It is noteworthy that the number of stars for each spectral type is neither uniform nor does it follow the initial mass function. It is typical for the spectral types to match MK anchor points,[5] rather than lie between them. For this reason, there are very few stars at F1 (24) compared to 915 and 881 at F0 and F2, respectively.

The results of the calibration are given in Table A.2, alongside the literature calibrations of Gray and Corbally (2009) and Adelman (2004). Figure 2.15 offers an easy comparison between the Gray and Corbally (2009) literature values and the values from this study.

The effect on the results of deficiencies in the method can be explained qualitatively, but a quantification of the differences compared to literature values is not possible because the literature values most likely suffer the same deficiencies. One such deficiency is the effect of stellar evolution on the findings. By selecting stars of luminosity class V only, the calibration uses stars across the whole main-sequence band, which is about one magnitude wide. Considerable dispersion therefore exists in the data.

The number of sources for spectral types is small, but those catalogues may contain stars classified by various classifiers. The extent to which they were checked by the authors is not certain. Even the best classifiers might disagree, use different sensitivity criteria, or make errors. While the lowest luminosity A0 star is going to be of class V, there is no guarantee that no class IV–V stars made it into the class V population, or even that the classifier actually distinguished between classes V and IV–V. Small luminosity class errors are easily made, particularly with noisy or low-resolution spectra (Gray, priv. comm.). Since medium to high-resolution spectra are usually degraded by convolving with a Gaussian for the purpose of spectral typing, the uncertainty on spectral subclass is not improved beyond 1–2 subclasses, as measured by agreement of different, standard diagnostics (Catanzaro et al. 2010).

[5] MK standards are divided into anchor points, primary, and secondary standards. Anchor points are those that have not changed since the initial definition of the system. See Appendix A of Gray and Corbally (2009).

Table A.2 Calibration of spectral type versus absolute magnitude (M_V)

Spectral type	M_V (Gray) (mag)	M_V (Adelman) (mag)	$\langle M_V \rangle$ Tycho (mag)	M_V Cubic (mag)	# of stars
B8	0.0		0.61	0.69	159
B8.5	0.4		0.72	0.83	77
B9	0.7		1.05	0.96	401
B9.5	1.0		1.20	1.09	193
A0	1.4	0.7	1.29	1.21	903
A1	1.6		1.45	1.33	553
A2	1.9	1.3	1.40	1.45	304
A3	2.0		1.49	1.56	307
A4			1.72	1.68	127
A5	2.1	2.0	1.67	1.80	153
A6	2.2	2.1	1.71	1.92	68
A7	2.3	2.3	1.92	2.04	111
A8	2.4	2.4	2.00	2.17	93
A9	2.5	2.5	2.44	2.31	331
F0	2.5	2.6	2.54	2.45	915
F1	2.8		2.55	2.60	24
F2	3.0		2.84	2.76	881
F3	3.1		2.96	2.94	1378
F4	3.3		2.79	3.12	46
F5	3.4		3.19	3.32	1678

Columns two and three are literature values from Gray and Corbally (2009) and Adelman (2004), respectively. Column four contains the mean value of M_V from this study of Tycho data, across the number of stars in that spectral-type bin as indicated in the right-most column. The fifth (penultimate) column contains the results of a cubic fit to those mean values, resulting in a more steady change of M_V with spectral type. The cubic-fit values are the ones plotted in Fig. 2.15

Using *Hipparcos* parallaxes offers precise data for a huge number of stars. The idea to limit the analysis to stars with parallaxes above 3 mas reduces the percentage error on the parallaxes used, but the brightness goes as $1/r^2$. A more conservative approach would be to use a higher parallax limit, even if it affords fewer stars for the analysis.

The stars used in this analysis were chosen to be normal and single. That the stars are single is clearly important for establishing the correct brightness, as is the contribution from background giants or optical pairs, but that is much harder to quantify. That the stars are normal is also important. The peculiar A stars rotate slowly, so by removing them the population that remains is rotating more quickly than the average A star. Faster rotating stars are gravity darkened around the equator (but gravity brightened at the poles —the flux has to go somewhere). Although this would appear to cancel out for randomly orientated rotational axes, one must consider that statistically there is a much larger solid angle (in latitude and longitude) from which a star appears to be 'equator on' than 'pole on'. Hence through gravity darkening,

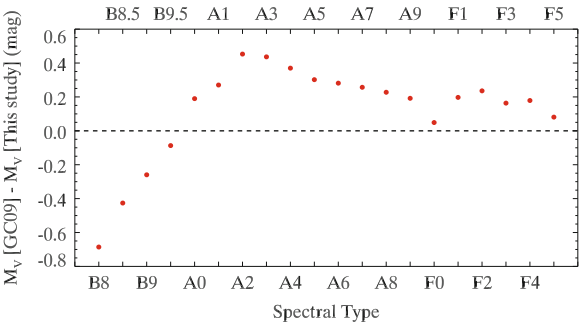

Fig. 2.15 Difference in M_V between Gray and Corbally (2009), "GC09", and this study, for each spectral type analysed

one expects the selection of normal stars (rapid rotators) to cause a systematic shift in brightness at spectral types where peculiar stars are most common: around A0 for the Ap stars and around A8 for the Am stars. It is not clear how literature calibrations have treated the chemically peculiar stars and binaries.

A future study to calibrate the main sequence using similar data would utilise the precise $B - V$ values, which are continuous, unlike the discrete spectral types, and a new calibration would be drawn for the bottom of the main-sequence band (i.e. the zero age main sequence) as was done in the seventies by Crawford (1975, 1978, 1979).

Appendix B: Angular Momentum Transfer

In this appendix we shall discuss the effect of transferring angular momentum between orbit and rotation, and show that large changes in rotational velocity can occur with relatively small corresponding changes in orbital separation.

B.1 Orbital Angular Momentum

For two stars of masses m_1 and m_2 treated as point masses in a circular orbit, the orbital angular momentum of the system is

$$L = L_1 + L_2 = m_1 v_1 r_1 + m_2 v_2 r_2 \tag{2.1}$$

where v and r denote the orbital velocities and orbital radii. Let us adopt the simplest scenario, where the two stars are identical. Equation 2.1 simplifies to

$$L = 2 m v_{\mathrm{orb}} r.$$

We must remember that each star orbits the barycentre of the system, which lies at the midpoint of the line connecting the two stars. Let us eliminate the orbital velocity

$$L = 2m\frac{2\pi r}{P}r = 4\pi m r^2 P^{-1} \quad (= 2m\omega r^2)$$

and by considering that the orbit is Keplerian, eliminate the period

$$L_{\rm orb} = 4\pi m r^2 \left(\frac{4\pi^2 r^3}{2Gm}\right)^{-1/2} = (8Gm^3 r)^{1/2}. \tag{2.2}$$

B.2 Rotational Angular Momentum

For the rotational angular momentum, let us assume the star has a uniform density. We shall focus on a single star when analysing the effect of orbital braking. The angular momentum of that star is:

$$L_{\rm rot} = I\omega = \frac{2}{5}mR^2\omega = \frac{2}{5}mRv_{\rm rot} \tag{2.3}$$

where R is the stellar radius.

B.3 Transfer of Momentum

We have assumed that both stars are identical, and now we shall assume that $m = 2\,{\rm M}_\odot$ and $R = 2\,{\rm R}_\odot$. We can derive an expression for the transfer of momentum between rotation and orbit, in either direction, by considering Eqs. 2.2 and 2.3.

$$\Delta L_{\rm orb} = \Delta L_{\rm rot}$$

$$(8Gm^3)^{1/2}\Delta r^{1/2} = \frac{2}{5}mR\Delta v_{\rm rot}$$

and substituting our assumed stellar parameters

$$80\Delta r^{1/2} \approx \Delta v_{\rm rot}. \tag{2.4}$$

This implies that for a reduction in rotational velocity of $10\,{\rm km\,s^{-1}}$, the orbital radius would have to increase by $\sim 10^4$ m. For a hypothetical 10-d orbit, whose radius is $\sim 10^{10}$ m, the fractional increase in orbital radius is only 10^{-6}, while the rotational velocity will have reduced by 10 % if the star were initially rotating at $100\,{\rm km\,s^{-1}}$. That is, substantial braking can occur without large changes in orbital radius.

What then happens when the orbit shrinks, as main-sequence binary orbits are often observed to do? The dominant orbital shrinkage mechanisms are not the reverse of the dominant rotational angular momentum changes. Instead, the orbital decay is driven by cases of mass loss where the secondary collects the mass lost from the primary. Roche-lobe overflow, for instance, causes large changes in the orbit over short time-scales, and not all mass lost is necessarily accreted onto the secondary. Even the angular momentum loss from a stellar wind, where total mass lost is small, will be effective for reducing the orbital period, and on yet longer time-scales gravitational-wave radiation plays a (smaller) role (Hilditch 2001).

References

Abt HA (1967) In: Cameron RC (ed) in Magnetic and Related Stars. p 173
Abt HA, Morrell NI (1995) ApJS 99:135
Abt HA (1961) ApJS 6:37
Abt HA, Hunter JH Jr (1962) ApJ 136:381
Abt HA, Levy SG (1978) ApJS 36:241
Abt HA (1979) ApJ 230:485
Abt HA, Levato H, Grosso M (2002) ApJ 573:359
Abt HA (2004) In: Maeder A, Eenens P, (ed) in IAU Symposium, Vol. 215, Stellar Rotation, ASP, pp 154-+
Abt HA, Boonyarak C (2004) ApJ 616:562
Abt HA, Willmarth D (2006) ApJS 162:207
Abt HA (2009) AJ 138:28
Adelman SJ (2004) In: Zverko J, Ziznovsky J, Adelman SJ, Weiss WW (eds) in IAU symposium, Vol. 224, The A-star puzzle pp 1–11
Babcock HW (1949) The Observatory 69:191
Baglin A, Breger M, Chevalier C, Hauck B, Le Contel JM, Sareyan JP, Valtier JC (1973) A&A 23:221
Balona LA (2011) MNRAS 415:1691
Balona LA (2013) MNRAS 431:2240
Bessell MS (1979) PASP 91:589
Braithwaite J (2008) Contrib Astron Obs Skalnate Pleso 38:179
Braithwaite J et al (2010) Highlights of Astron 15:161
Catanzaro G, Frasca A, Molenda-Żakowicz J, Marilli E (2010) A&A 517:A3
Conti PS (1965) ApJ 142:1594
Crawford DL (1975) AJ 80:955
Crawford DL (1978) AJ 83:48
Crawford DL (1979) AJ 84:1858
Debernardi Y (2000) In: Reipurth B, Zinnecker H (eds) in IAU symposium, Vol. 200, IAU symposium on the formation of binary stars ASP conference series, p. 161
Debernardi Y, Mermilliod J-C, Carquillat J-M, Ginestet N (2000) A&A 354:881
Degroote P et al (2011) A&A 536:A82
Deutsch AJ (1956) PASP 68:92
Erspamer D, North P (2003) A&A 398:1121
Fitzgerald MP (1970) A&A 4:234
Glebocki R, Gnacinski P, Stawikowski A (2000) Acta Astron. 50:509
Gray RO, Corbally JC (2009) Stellar spectral classification. Princeton University Press, Princeton
Hartoog MR (1977) ApJ 212:723

Hilditch RW (2001) An introduction to close binary stars. CUP, Cambridge
Houk N, Cowley AP (1975) University of Michigan catalogue of two-dimensional spectral types for the HD stars. volume I. Declinations −90_ to −53°. University of Michigan, Michigan
Houk N (1978) Michigan catalogue of two-dimensional spectral types for the HD stars. University of Michigan, Michigan
Houk N (1982) Michigan catalogue of two-dimensional spectral types for the HD stars. Volume_3. Declinations −40° to −26°. University of Michigan, Michigan
Houk N, Smith-Moore M (1988) Michigan catalogue of two-dimensional spectral types for the HD stars. Volume 4, declinations −26° to −12°. University of Michigan, Michigan
Houk N, Swift C (1999) Michigan catalogue of two-dimensional spectral types for the HD stars; vol. 5. University of Michigan, Michigan
Hubrig S, North P, Mathys G (2000) ApJ 539:352
Hubrig S, North P, Medici A (2000) A&A 359:306
Hubrig S, North P, Schöller M, Mathys G (2006) Astron Nachr 327:289
Hubrig S, North P, Schöller M (2007) Astron Nachr 328:475
Irwin J, Bouvier J (2009) In: Mamajek EE, Soderblom DR, Wyse RFG (eds) in IAU symposium, Vol. 258, IAU symposium. CUP, pp 363–374
Jaschek C, Conde H, de Sierra AC (1964) Obs Astron La Plata Ser Astron 28:1
Jaschek C, Gomez AE (1998) A&A 330:619
Joshi S, Mary DL, Martinez P, Kurtz DW, Girish V, Seetha S, Sagar R, Ashoka BN (2006) A&A 455:303
Kennedy PM (1983) MK Classication Catalog Extension. Weston Creek: Mt. Stromlo & Siding Spring Obs
Kochukhov O, Bagnulo S (2006) A&A 450:763
Kogure T (1981) PASJ 33:399
Kouwenhoven MBN, Brown AGA, Zinnecker H, Kaper L, Portegies Zwart SF (2005) A&A 430:137
Kraft RP (1967) ApJ 150:551
Landstreet JD, Barker PK, Bohlender DA, Jewison MS (1989) ApJ 344:876
Landstreet JD, Mathys G (2000) A&A 359:213
Langer N (2009) A&A 500:133
Leroy JL, Bagnulo S, Landolfi M, Landi Degl'Innocenti E (1994) A&A 284:174
Marcy GW, Benitz KJ (1989) ApJ 344:441
Mason BD, Gies DR, Hartkopf WI, Bagnuolo WG Jr, ten Brummelaar T, McAlister HA (1998) AJ 115:821
Mathys G (2004) In: Maeder A, Eenens P (eds) in IAU Symposium, Vol. 215, Stellar Rotation., ASP, p 270
Mathys G, Hubrig S, Landstreet JD, Lanz T, Manfroid J (1997) A&AS 123:353
Mazeh T, Tamuz O, North P (2006) Ap&SS 304:343
Michaud G, Charland Y, Vauclair S, Vauclair G (1976) ApJ 210:447
Molenda-Żakowicz J. et al(2009) In: Guzik JA, Bradley PA (eds) in American Institute of Physics Conference Series, Vol. 1170, American Institute of Physics Conference Series pp 531–534
Moss D (1990) MNRAS 244:272
Murphy SJ, Grigahcène A, Niemczura E, Kurtz DW, Uytterhoeven K (2012) MNRAS 427:1418
North P (1993) In: Astronomical society of the pacific conference series, Vol. 44, IAU Colloq. 138: Peculiar versus Normal Phenomena in A-type and Related Stars, Dworetsky MM, Castelli F, Faraggiana R, (eds), ASP Conference Series, p. 577
North P (1984) A&A 141:328
North P (1985) A&A 148:165
North P (1998) A&A 334:181
North P, Ginestet N, Carquillat J-M, Carrier F, Udry S (1998) Contrib Astron Obs Skalnate Pleso 27:179

North P, Jaschek C, Hauck B, Figueras F, Torra J, Kunzli M (1997) In: ESA special publication, Vol. 402, Hipparcos - Venice '97, Bonnet RM, Høg E, Bernacca PL, Emiliani L, Blaauw A, Turon C, Kovalevsky J, Lindegren L, Hassan H, Bouffard M, Strim B, Heger D, Perryman MAC, Woltjer L (eds), pp. 239–244
Ochsenbein F, Bauer P, Marcout J (2000) A&AS 143:23
Preston GW (1970) In: Slettebak A (ed) in IAU colloq. 4: stellar rotation. Reidel Publishing Company p 254
Rieutord M (1992) A&A 259:581
Royer F (2009) The Rotation of Sun and Stars. in Lecture Notes in Physics. Springer Verlag, Berlin, pp 207–230
Royer F, Gerbaldi M, Faraggiana R, Gómez AE (2002a) A&A 381:105
Royer F, Grenier S, Baylac M-O, Gómez AE, Zorec J (2002b) A&A 393:897
Royer F, Zorec J, Gómez AE (2007) A&A 463:671
Royer F, Zorec J, Gómez AE (2004) In: IAU Symposium, Vol. 215, Stellar Rotation, Maeder A, Eenens P (ed) ASP, p. 154
Sills A, Pinsonneault MH, Terndrup DM (2000) ApJ 534:335
Slettebak A (1997) 1955, ApJ, 121:653
Smalley B, Dworetsky MM (1995) A&A 293:446
Smith MA (1973) ApJS 25:277
Stibbs DWN (1950) MNRAS 110:395
Stępień K (2000) A&A 353:227
Tassoul J-L, Tassoul M (1992a) ApJ 395:259
Tassoul M, Tassoul J-L (1992b) ApJ 395:604
Thompson SE et al (2012) ApJ 753:86
Uesugi A, Fukuda I (1982) Catalogue of stellar rotational velocities (revised). Department Of Astronomy, Kyoto Univ, Kyoto
Vauclair G (1976) A&A 50:435
Wade GA (1997) A&A 325:1063
Witte MG, Savonije GJ (2001) A&A 366:840
Wolff SC (1967) ApJS 15:21
Wolff SC (1983) The A-type stars: problems and perspectives. NASA SP-463
Wolff S, Simon T (1997) PASP 109:759
Wright CO, Egan MP, Kraemer KE, Price SD (2003) AJ 125:359
Zahn JP (1984) In: Maeder A, Renzini A (eds) in IAU symposium, Vol. 105, observational tests of the stellar evolution theory. Reidel Publishing Company, p 379
Zahn J-P (1975) A&A 41:329
Zahn J-P (1977) A&A 57:383
Zorec J, Royer F (2012) A&A 537:A120

http://www.springer.com/978-3-319-09416-8

Investigating the A-Type Stars Using Kepler Data

Murphy, S.J.

2015, XVII, 204 p. 121 illus., 73 illus. in color.,
Hardcover
ISBN: 978-3-319-09416-8